Dynamics of Concentrated Hard-Sphere Colloids Near a Wall

V. N. Michailidou and G. Petekidis*

FORTH/IESL and Department of Material Science & Technology, University of Crete, 71110, Heraklion, Greece

J. W. Swan and J. F. Brady

Division of Chemistry and Chemical Engineering, California Institute of Technology, Pasadena, California 91125, USA

(Received 19 July 2008; published 12 February 2009)

We investigate the Brownian motion of hard-sphere colloids near a solid wall by Evanescent Wave Dynamic Light Scattering (EWDLS). We carried out measurements for various volume fractions of sterically stabilized poly(methyl methacrylate) (PMMA) particles over a range of scattering wave vectors, $\mathbf{q}$. While in the dilute regime, the near wall short-time diffusion is significantly slowed down due to particle-wall hydrodynamic interactions (HI); as volume fraction increases, the wall effect is progressively diminished at all $\mathbf{q}$'s. We present a new analysis for the EWDLS short-time self- and collective diffusivities applicable to all volume fractions and a simple model for the self-diffusion describing the interplay between particle-wall and particle-particle HI. Moreover, a weaker decay of the near-wall self-diffusion coefficient with volume fraction is predicted by Stokesian dynamics simulations.

DOI: 10.1103/PhysRevLett.102.068302 PACS numbers: 82.70.Dd, 47.57.−s, 68.35.Fx, 78.35.+c

Interfaces are an important ingredient of soft matter and biological systems [1]. Consequently, Brownian motion of colloidal particles, polymer chains or proteins, near surfaces, is of central importance, determines their macroscopic properties and impacts their biological functions. Such confined dynamics are affected by direct energetic interactions as well as excluded volume and hydrodynamic interactions. The latter affect diffusion and flow of particles near a hard wall [2,3], between two surfaces [4] or in microfluidic channels [5]. In biological systems, they play an essential role in collective motion of sperm cells near interfaces [6] and swimming bacteria in thin films [7]. Confined flows of colloidal suspensions are also ubiquitous in industrial processes from food processing to petrol recovery [8]. Thus, near-wall Brownian motion is of interest both for fundamental mesoscopic physics and interface science as well as for its high technological relevance such as in microfluidics and optofluidics [9]. A key question is how particle dynamics are affected by the existence of nonpenetrable walls via hydrodynamic interactions (HIs).

Experimentally, optical microscopy [10] limited by particle size, and evanescent wave dynamic light scattering (EWDLS) [2,11], combining dynamic light scattering (DLS) with the short penetration depth of an evanescent wave under total internal reflection conditions, have been used to study near surface dynamics. The latter requires a careful interpretation of the intensity time-autocorrelation function. Currently, only its initial decay from dilute suspensions is well described taking into account anisotropic diffusion and the evanescent wave illumination [11]. EWDLS has been used to study dynamics of polymer brushes, particles near a brush and rodlike polymers near a wall [12]. With increasing volume fraction (ϕ) particle-particle HIs become important and modify the wall-induced drag effect. Furthermore, liquid to solid transitions in confinement are related with modified particle mobility near a wall [13]. However, near-wall dynamics in concentrated suspensions are virtually unexplored both experimentally and theoretically.

In this Letter, we employ dynamic light scattering in bulk (3D) and near a hard wall (quazi-2D) to compare for the first time the corresponding dynamics at a wide range of volume fractions and further use a simple model together with Stokesian Dynamics Simulations to capture the basic physics involved. We conducted EWDLS experiments and conventional DLS (with a normal setup) at several scattering wave vectors, q $[=(4\pi n_2/\lambda_0)\times \sin(\theta_s/2)]$, where n_2 $(=1.497)$ is the suspension refractive index, λ_0 $(=532$ nm) the laser wavelength, and θ_s the scattering angle. The evanescent wave was generated at the interface of a semicylindrical prism of high refractive index ($n_1 = 1.627$) with the suspending liquid confined in an attached cell. At total internal reflection, the inverse penetration depth is $\kappa/2$ $[=(2\pi n_1/\lambda_0)\sqrt{\sin^2\theta_i - \sin^2\theta_c}]$, where θ_i is the incident angle and θ_c $(=67.9°)$ the measured critical angle. The cell was placed at the center of a θ–2θ goniometer enabling variation of both q $(1 < qR < 7)$ and $\kappa/2$ $[1 < 2/(\kappa R) < 6]$.

The suspensions were composed of sterically stabilized (with a thin poly-12-hydrohystearic acid layer) poly (methyl methacrylate) (PMMA) nearly hard-sphere particles with radius $R = 183$ nm (and $R = 154$ nm and 118 nm for the two higher ϕ's, determined by light scattering) suspended in a refractive index matching tetralin/cis-decalin (30%/70%) mixture to minimize multiple scattering. We prepared several volume fractions by diluting a concentrated batch. Its volume fraction was determined in the coexistence regime [14] (for the 154 and 118 nm

particles random close packing of 0.65 was used instead due to polydispersity). We measured the normalized intensity time-autocorrelation function (TCF)[14], $g^{(2)}(\mathbf{q}, t; \kappa) = \langle I(\mathbf{q}, t; \kappa) I(\mathbf{q}, 0; \kappa)\rangle / \langle I(t)\rangle^2$, of the light scattering intensity, $I(\mathbf{q}, t; \kappa)$, at room temperature ($T = 18\,^{\circ}\mathrm{C}$), under homodyne conditions in 3D and mixed homodyne-heterodyne in EWDLS due to strong static scattering from the prism surface. We calculated the normalized field autocorrelation function, $f(\mathbf{q}, t; \kappa) = \langle E(\mathbf{q}, t; \kappa) E^*(\mathbf{q}, 0; \kappa)\rangle / \langle I\rangle$ from $g^{(2)}(\mathbf{q}, t; \kappa)$, using the normal (3D) or modified (EWDLS) Siegert relation [11] and further computed its initial decay rate [14], $\Gamma = -\frac{\partial}{\partial t} \times \ln f(\mathbf{q}, t; \kappa)$ as $t \to 0$, to determine the q dependent short-time diffusion coefficient, $D(\phi, \mathbf{q}, \kappa) = \Gamma / q^2$.

In EWDLS, the incident beam intensity decays exponentially with distance from the boundary and thus the typical DLS averages [14,15] are modulated accordingly. In this case, $D^{2D}(\phi, \mathbf{q}, \kappa) = \Gamma / (\mathbf{k} \cdot \mathbf{k}^*)$ where $\mathbf{k} = \mathbf{q} + \mathbf{e}_3 i\kappa/2$ and $\mathbf{e}_3$ is a vector normal to the wall pointing into the fluid. Thus, we have redefined the scattering vector for an evanescent wave as the sum of the usual $\mathbf{q}$ and an imaginary component that gives rise to the exponential decay. Following typical DLS analysis, we can recover the ''evanescent'' short-time collective and self-diffusivity. For $qR \to 0$, we can show [16] that the decay of $f(\mathbf{q}, t; \kappa)$ measures the collective diffusivity as

$$D_C^{2D}(\phi, \kappa) = \frac{\langle D_{33}^{\alpha\alpha} e^{-\kappa z_\alpha} + (N-1) D_{33}^{\alpha\beta} e^{-(\kappa/2)(z_\beta + z_\alpha)}\rangle}{\langle e^{-\kappa z_\alpha} + (N-1) e^{-(\kappa/2)(z_\beta + z_\alpha)}\rangle} \tag{1}$$

where, in an ensemble of N particles, $D_{33}^{\alpha\alpha}$ ($= kTM_{33}^{\alpha\alpha}$) and $D_{33}^{\alpha\beta}$ ($= kTM_{33}^{\alpha\beta}$) are products of the thermal energy with the perpendicular to the wall self hydrodynamic mobility of one particle and that of a pair of particles, respectively, with z_α and z_β their distances from the wall. Hence, the ''evanescent'' collective diffusivity, $D_C^{2D}(\phi, \kappa)$, probes diffusion only perpendicular to the wall since motion parallel to the wall is $O(qR)$ while perpendicular is $O(1)$.

In contrast, at large qR, the decay of $f(\mathbf{q}, t; \kappa)$ measures a weighted average of parallel and perpendicular ''evanescent'' short-time self-diffusivities as

$$D_S^{2D}(\phi, \kappa) = \frac{\langle [q_\parallel^2 D_{11}^{\alpha\alpha} + (q_\perp^2 + \frac{\kappa^2}{4}) D_{33}^{\alpha\alpha}] e^{-\kappa z_\alpha}\rangle}{(q_\parallel^2 + q_\perp^2 + \frac{\kappa^2}{4}) \langle e^{-\kappa z_\alpha}\rangle} \tag{2}$$

where $D_{11}^{\alpha\alpha}$ ($= kTM_{11}^{\alpha\alpha}$) reflects the self hydrodynamic mobility parallel to the wall. In particular, for $\kappa/2 \ll q$ (holding here) and $q_\parallel \sim q_\perp$ (at $\theta_s \sim 90^{\circ}$), the short-time decay of $f(\mathbf{q}, t; \kappa)$ weighs equally the parallel and perpendicular components, yielding $D_S^{2D}(\phi, \kappa) = \langle (D_{11}^{\alpha\alpha} + D_{33}^{\alpha\alpha}) e^{-\kappa z_\alpha}\rangle / 2\langle e^{-\kappa z_\alpha}\rangle$. These results are similar (and reduce as $\phi \to 0$) to the cumulant expansion of Holmqvist *et al.* [11], but apply not only in the dilute regime, but over the entire range of ϕ' s.

We first present data for both DLS and EWDLS from suspensions of increasing ϕ to reveal the effect of particle crowding on wall-induced HIs. Figure 1 shows $f(\mathbf{q}, t; \kappa)$ at $qR = 4.58$ ($q_\parallel \sim q_\perp$) for a dilute and a concentrated suspension. For all EWDLS data, the penetration depth was $2/\kappa = 4.49R$ ($\theta_i = 68.22^{\circ}$). While in the dilute suspension the quazi-2D dynamics are clearly slower due to wall-induced drag [2,17], in concentrated suspensions, the quazi-2D and 3D dynamics are essentially the same, especially for short times. This reveals a qualitative modification of the wall-induced HIs at high ϕ as compared to the dilute limit.

In Fig. 2, we show the q-dependent diffusivity deduced from the short-time decay of $f(\mathbf{q}, t; \kappa)$ in both 3D and quazi-2D, normalized by the Stokes-Einstein-Sutherland diffusivity, $D_0 = kT/(6\pi\eta R)$. At high ϕ's, the slowing of the dynamics near the peak of the structure factor [14] is evident both in quazi-2D and the 3D. To quantify the influence of ϕ on the dynamics, one should extract the short-time collective- and self-diffusivity in the limits of $qR \to 0$ and high qR's [where $S(q) = 1$], respectively. While the former entails large errors, especially for near-wall data, for the latter, we determine $D(\phi, \mathbf{q}, \kappa)$ at $qR = 4.58$ where the parallel and perpendicular diffusivities are averaged in the ratio of one to one. In 3D, $D(qR = 4.58)$, which to a good approximation may be identified as the self-diffusivity [18], agrees well with Stokesian dynamics simulations with full HI [19] (Fig. 3) providing further support for its self-diffusion character [20].

In Fig. 3, we also show the ϕ dependence of the near-wall self-diffusivity (again at $qR = 4.58$). At $\phi \to 0$, we recover a ratio of near-wall to bulk self-diffusivity of 0.68 (at $2/\kappa = 4.49R$) in agreement with the anticipated near-wall hydrodynamic slowing down [11,17]. In the same figure, we show indicatively the 3D and near-wall collective diffusivities from linear fits at low q's for few high ϕ's. Both in 3D and quazi-2D, the collective dynamics become

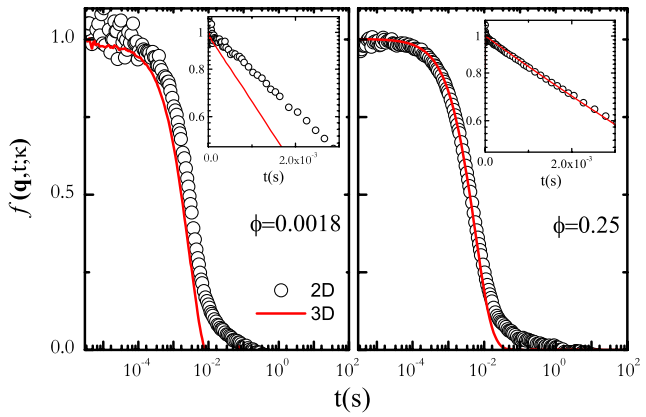

FIG. 1 (color online). $f(\mathbf{q}, t; \kappa)$ from DLS (3D) and EWDLS (quazi-2D) at $qR = 4.58$ (and $2/\kappa = 4.37R$ in the latter case) for a dilute ($\phi = 0.0018$) and a concentrated suspension ($\phi = 0.25$). The insets portray the initial decay of these functions.

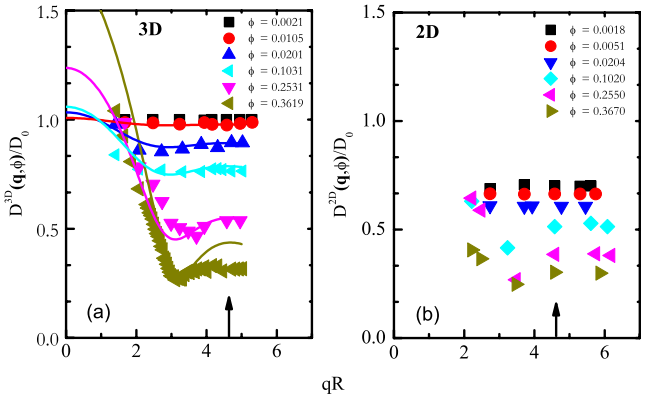

FIG. 2 (color online). Normalized q-dependent diffusivity as a function of qR in 3D and quazi-2D for several φ's. The arrow denotes the qR where $q_{\parallel} \sim q_{\perp}$ ($\theta_s \sim 90°$) and the lines denote the theoretical predictions of Beenaker and Mazur [24] for diffusion in 3D.

faster with increasing ϕ, under the influence of osmotic compressibility [decrease of $S(q \to 0)$] while single particle dynamics become slower due to hydrodynamic interactions [14]. However, above $\phi \sim 0.35$, the near-wall dynamics at all q, below and above the peak of $S(q)$, are virtually indistinguishable from those in 3D {see supplementary material for $D(Q)$ vs q at high ϕ [21]}. Consequently, the decrease of self-diffusivity with ϕ near the wall is weaker than in 3D, whereas, although not accurately determined, the opposite trend is suggested for the collective diffusivity which increases with ϕ stronger than in 3D.

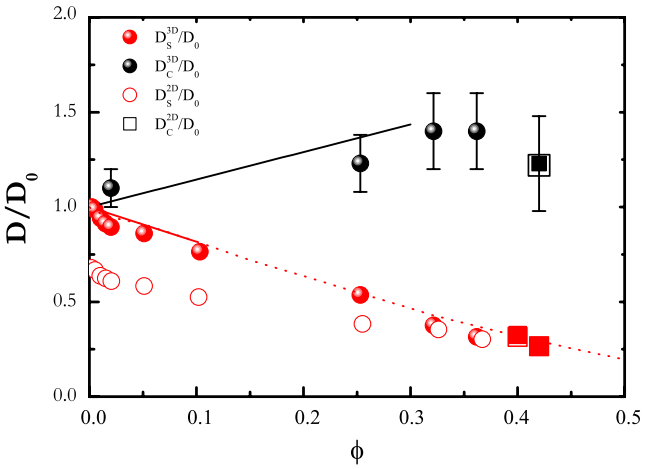

FIG. 3 (color online). The ϕ-dependence of the short-time collective, D_C, and self, D_S, diffusivity, in 3D and near the wall normalized by the Stokes-Einstein-Sutherland diffusivity D_0. The errors in D_C result from the extrapolation to $q = 0$. The last two points (squares) were measured with $R = 154$ nm ($\phi = 0.4$) and 114 nm ($\phi = 0.42$) particles. The solid lines correspond to Batchelor's dilute predictions for the collective and self-diffusion [23] while the dashed line is the Stokesian dynamics prediction for self-diffusion [19].

A simple model explains the physical origin of the diminished effect of the wall at high ϕ. The decrease in the short-time self-diffusivity with ϕ is caused by HIs comprising of a far-field ($\sim 1/r$) and a near-field (lubrication) contribution [19]. The particle-wall and particle-particle near-field HI may be reasonably assumed the same (they have the same singular behavior near contact). Thus, at high concentrations and over short distances, a particle does not feel if it is close to a wall or to a second particle. We use this idea to calculate the ratio of 3D to quazi-2D self-diffusivity. In 3D, we write the normalized diffusivity as $D_S^{3D}(\phi) = (\eta_{ff}^{3D} + \eta_{lub}^{3D})^{-1}$ and $D_{ff}^{3D}(\phi) = (\eta_{ff}^{3D})^{-1}$, with ff and lub denoting the far- and near-field HI, respectively, yielding $\eta_{lub}^{3D} = 1/D_S^{3D}(\phi) - 1/D_{ff}^{3D}(\phi) = \eta_{lub}^{2D}$. For a given penetration depth and for a dense suspension, the near-wall self-diffusivity may be written as $D_S^{2D}(\phi, \kappa) = (\eta_{ff}^{2D} + \eta_{lub}^{3D})^{-1}$. We further assume that the far-field contribution to the near-wall self-diffusivity has the same ϕ-dependence as in 3D, and thus $D_{ff}^{2D}(\phi, \kappa) = D_{ff}^{3D}(\phi)(D_0^{2D}(\kappa)/D_0)$. The above yields a ratio,

$$\frac{D_S^{3D}(\phi)}{D_S^{2D}(\phi, \kappa)} = 1 + \left(\frac{D_S^{3D}(\phi)}{D_{ff}^{3D}(\phi)}\right)\left(\frac{D_0}{D_0^{2D}(\kappa)} - 1\right). \quad (3)$$

The right-hand side of Eq. (3) is determined using the experimental dilute limit $D_0/D_0^{2D}(\kappa)$ and the ratio $D_S^{3D}(\phi)/D_{ff}^{3D}(\phi)$ taken from simulations [19]. As seen in Fig. 4(a), the above equation predicts the observed merging of 3D and quazi-2D dynamics with increasing ϕ suggesting that the proposed mechanism is broadly valid, although the quantitative discrepancy at high ϕ's calls for detailed calculations of many particle near-wall HIs that may enhance the phenomenon.

The ϕ dependence of the quazi-2D self-diffusivity is also very interesting. We have already observed a weaker decay of the near-wall diffusivity compared to 3D (Fig. 3). We further used Stokesian dynamics simulations [22] to calculate the order ϕ term in the virial expansion of $D_S^{2D}(\phi, \kappa)$. In 3D, Batchelor predicts [23] that $D_S^{3D}(\phi) = D_0(1–1.83\phi)$. Near the wall, however, the coefficient depends on the penetration depth so that

$$D_S^{2D}(\phi, \kappa) = D_0^{2D}(\kappa)(1 - \alpha(\kappa)\phi). \quad (4)$$

$\alpha(\kappa)$ was calculated by averaging HIs over all possible positions of a second particle around a first one (placed at distance z from the wall). Then this average was integrated over the height of the first particle above the wall weighted exponentially, akin to the EWDLS ensemble average. Figure 4(b) shows $D_0^{2D}(\kappa)/D_0$ and $\alpha(\kappa)$ from simulations together with the experimental values at $2/\kappa = 4.37R$. The results from simulations and experiments are in very good agreement for $D_0^{2D}(\kappa)/D_0$ while the experimental $\alpha(\kappa)$ is clearly smaller than 1.83 as predicted by simulations for all

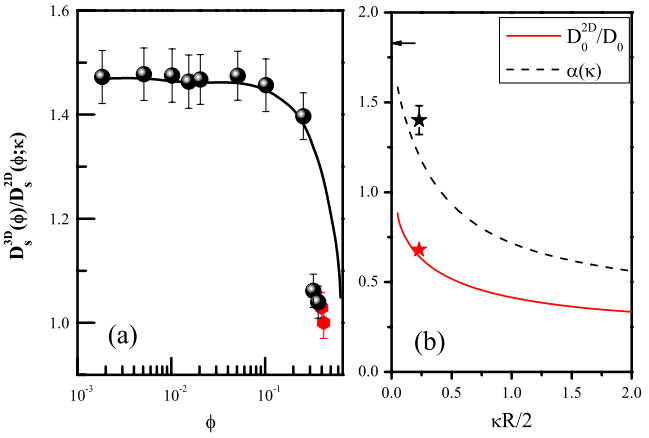

FIG. 4 (color online). (a) The ratio of 3D to the near-wall self-diffusivity as a function of volume fraction. The last two points were measured with $R = 154$ nm and $R = 118$ nm particles. The line corresponds to the simple model prediction [Eq. (3)]. (b) Dilute limit quazi-2D short-time self-diffusion and order ϕ coefficient from Stokesian dynamics simulations. The stars represent experimental data, and the arrow corresponds to Batchelor's order ϕ prediction [23] in 3D (i.e., 1.83).

values of κ. This suggests that the wall screens out HIs among many particles in the dilute limit, reminiscent of the weaker decay of HIs near the wall $1/r^2$ versus $1/r$ in 3D.

Concluding, we have shown that hard-sphere particle dynamics near a wall are significantly altered as ϕ is increased. The hydrodynamic drag that slows a particle in the vicinity of the wall is progressively weakened at high ϕ due to a counterbalancing of the wall particle by particle-particle HIs. The wall is then felt as another, larger particle. While the convergence of near-wall and bulk dynamics at high ϕ is observed generically in both collective and self-diffusion, we have provided a simple model to describe the behavior of the short-time self-diffusion coefficient and further calculate the order ϕ contribution to a virial expansion of $D_S^{2D}(\phi, \kappa)$ from Stokesian dynamics simulations. The latter is found to be smaller than Batchelor's prediction in 3D due to the screened HIs between particle pairs adjacent to a wall. Moreover, experimental data suggest that near-wall collective diffusivity exhibits a stronger growth with ϕ than in 3D. The study of the near-wall HIs on the collective diffusivity, the ϕ-dependence of the parallel and perpendicular diffusivities, as well as an understanding of the long-time, near-wall dynamics will be the subjects of future work.

We thank A. Schofield for providing the colloids and J. Dhont and P. Lang for discussions and a measurement in the Julich EWDLS setup (with the 154 nm sample). We acknowledge funding from GSRT (PENED-03E△566), NSF NIRT Grant No. (CBET 0506701) and EU Grants "Cosines" (MTCD-CT-2005-029944) and "SoftComp" (NMP3-CT-2004-502235).

*georgp@iesl.forth.gr

[1] J. Lyklema, *Fundamentals of Interface & Colloid Science* (Academic Press, New York, 1995).
[2] K. H. Lan *et al.*, Phys. Rev. Lett. **57**, 17 (1986); L. Lobry and N. Ostrowsky, Phys. Rev. B **53**, 12050 (1996).
[3] T. M. Squires and M. P. Brenner, Phys. Rev. Lett. **85**, 4976 (2000).
[4] R. Pesche and G. Nagele, Phys. Rev. E **62**, 5432 (2000).
[5] T. Beatus *et al.*, Phys. Rev. Lett. **99**, 124502 (2007); B. Cui *et al.*, Phys. Rev. Lett. **89**, 188302 (2002).
[6] I. H. Riedel *et al.*, Science **309**, 300 (2005).
[7] S. Andrey *et al.*, Phys. Rev. Lett. **98**, 158102 (2007).
[8] W. B. Russel, D. A. Saville, and W. R. Schowalter, *Colloidal Dispersions* (Cambridge University Press, Cambridge, England, 1989).
[9] G. M. Whitesides *et al.*, Phys. Today **54**, No. 6, 42 (2001); D. Psaltis *et al.*, Nature (London) **442**, 381 (2006).
[10] M. D. Carbajal-Tinoco *et al.*, Phys. Rev. Lett. **99**, 138303 (2007).
[11] P. Holmqvist *et al.*, Phys. Rev. E **74**, 021402 (2006); J. Chem. Phys. **126**, 044707 (2007).
[12] G. Fytas *et al.*, Science **274**, 2041 (1996); G. E. Yakubov *et al.*, Phys. Rev. Lett. **92**, 115501 (2004); E. Filippidi *et al.*, Langmuir **23**, 5139 (2007); B. Loppinet *et al.*, Langmuir **14**, 4958 (1998).
[13] C. R. Nugent *et al.*, Phys. Rev. Lett. **99**, 025702 (2007).
[14] P. N. Pusey, in *Colloidal Suspensions in Liquids, Freezing and the Glass Transition*, Proceedings of the Les Houches Summer School, edited by J. P. Hansen, D. Levesque, and J. Zinn-Justin (Elsevier, Amsterdam, 1991).
[15] J. F. Brady, J. Fluid Mech. **272**, 109 (1994).
[16] J. W. Swan *et al.* (to be published), see also Ref. [21] for details.
[17] H. Faxén, Ark. Mat. Astron. Fys. **17**, 1 (1923); H. Brenner, Chem. Eng. Sci. **16**, 242 (1961).
[18] P. N. Segre *et al.*, Phys. Rev. E **52**, 5070 (1995).
[19] R. J. Phillips *et al.*, Phys. Fluids **31**, 3462 (1988); A. J. Banchio and J. F. Brady, J. Chem. Phys. **118**, 10323 (2003).
[20] Although in theory at $qR = 4.6$ [near the first $S(q)$ minimum] $D(q)$ is enhanced relative to self-diffusion, experimentally we find small variations of $D(q)$ above $qR = 4$.
[21] See EPAPS Document No. E-PRLTAO-102-049909 for supplementary material. For more information on EPAPS, see http://www.aip.org/pubservs/epaps.html.
[22] J. W. Swan and J. F. Brady, Phys. Fluids **19**, 113306 (2007).
[23] G. K. Batchelor, J. Fluid Mech. **74**, 1 (1976).
[24] C. W. J. Beenaker and P. Mazur, Physica A (Amsterdam) **126**, 349 (1984).